

Low Cost 3D-Printed Biosensor Arrays for Protein-based Cancer Diagnostics based on Electrochemiluminescence

James F. Rusling^{1,2,3,4}, Karteek Kadimisetty¹, Spundana Malla¹,
Gregory W. Bishop¹ and Jennifer E. Satterwhite-Warden¹

¹Department of Chemistry, University of Connecticut, Storrs, Connecticut 06269-3060, U.S.A.

²Institute of Materials Science, University of Connecticut, Storrs, Connecticut 06269-3136, U.S.A.

³Department of Surgery and Neag Cancer Center, University of Connecticut Health Center,
Farmington, Connecticut 06030, U.S.A.

⁴School of Chemistry, National University of Ireland at Galway, Galway, Ireland

Keywords: 3D-Printing, Cancer, Multiplexed Protein Detection, Microfluidics, Immunoarray.

Abstract: Development and fabrication of bioanalytical devices by 3D printing offers revolutionary new routes to low cost clinical diagnostic devices for molecular measurements. Relevant to future protein-based cancer diagnostics, we describe and review here our recent development of prototype protein immunoarray devices using desktop Fused Deposition Modeling (FDM) and stereolithographic 3D printers. All these system feature sensitive electro-optical detection by a method called electrochemiluminescence (ECL). Our first 3D-printed immunoarray features screen-printed sensors in which manual manipulations enable gravity flow reagent delivery for measurement of 3 proteins at detection limits of 0.3 to 0.5 pg/mL. ECL detection is achieved in an open channel on integrated disposable screen-printed sensor elements. We then address the issue of printing and processing optically clear plastic using a stereolithographic printer to build a closed ECL detection chamber. Finally, we describe a prototype 3D-printed microprocessor-controlled enclosed microfluidic ECL immunoarray featuring reagent reservoirs, micropumps and clear plastic detection chamber with printed nanowells for ECL emission.

1 INTRODUCTION

Desktop 3D printers offer unprecedented new options to design and fabricate low cost, high performance biosensors (Gross, B.C., et al., 2014). Development of microfluidic sensing devices by 3D-printing can provide rapid computer-based design prototyping and testing, avoiding the necessity for masks or templates used in more traditional approaches such as lithography. Design-to-device fabrication can be rapidly achieved with 3D-printers, and devices can be produced cheaply without the need for economies of scale. Recent examples include 3D printed systems for monitoring metal ions (Su et al., 2014) and add-ons for turning smartphones into food allergen sensors (Coskun & Wang, et al., 2013; Wei, Nagi, et al., 2014; Coskun & Nagi, et al., 2013; Roda et al., 2014; Wei, Luo, et al., 2014). Electrochemical sensing was integrated into 3D-printed fluidic devices for dopamine, nitric oxide (Erkal et al., 2014) and hydrogen peroxide (Bishop et al., 2015). Biological and diagnostic

applications have recently been reviewed (O'Neill, et al. 2014; Meng, et al. 2015).

There is a high level of interest in the medical community for measuring levels of multiple biomarker proteins for cancer diagnostics (Hanash, et al., 2011). Measuring biomarker proteins in conjunction with genomic analysis of patients and their cancers are expected to help usher in a new era of *Precision Medicine* (Kohane, 2015). Serum levels of *proteins* are biomarkers that can serve to indicate the onset, existence or progression of cancer (Hanash, et al., 2011, Rusling, et al., 2011). Measurement of panels of protein biomarkers holds enormous potential for early cancer detection as well as personalized cancer therapy and treatment monitoring. However, these applications have yet to be broadly realized in a form that can be readily adapted to point-of-care. For such diagnostic strategies to reach widespread clinical or point-of-care (POC) use, low cost, sensitive, easy to use devices are needed to measure multiple biomarker proteins in patient serum (Rusling, et al. 2010).

Enzyme-linked immunosorbent assay (ELISA) is the gold standard for clinical protein assays with DLs as low as 1-3 pg/mL, but with limitations in sensitivity, analysis time, multiplexing, and sample size. Newer commercial multiprotein detection systems are very useful for research, and rely on expensive, technically demanding instrumentation difficult to implement in the clinic (Hanash, et al., 2011, Rusling, et. al., 2011). These approaches rarely achieve detection below pg mL⁻¹ levels, while some biomarker proteins have serum levels well below 1 pg mL⁻¹.

In this paper, we describe new approaches to develop 3D-printed multiplexed protein immunoassay devices using a sensitive electro-optical detection method called electrochemiluminescence (ECL) (Forster, et al., 2009). Detection employs an ECL-active dye that can be loaded into nanoparticle labels, and electrochemically active co-reactant, and applied voltage to produce visible ECL light detected by a charge-coupled device (CCD) camera. Below we describe a prototype 3D-printed immunoassay system with screen-printed sensors in which manual manipulations are used to enable gravity flow reagent delivery for the detection of 3 proteins. This system uses ECL detection in an open channel without a window in front of the sensor elements. We then address the issue of printing and processing optically clear plastic to build a closed chamber that will emit ECL light. Finally, we present a prototype 3D-printed microprocessor-controlled microfluidic ECL immunoarray featuring reagent reservoirs and clear plastic detection chamber with printed nanowells for ECL emission.

2 RESULTS

2.1 Gravity-flow Immunoarray

A prototype protein immunoarray was fabricated using the desktop Fused Deposition Modeling (FDM) 3D printer MakerBot Replicator 2X and polylactic acid (PLA). This device (Figure 1) features an open channel housing a screen-printed electrode array insert powered by a supercapacitor for ECL generation detected by a CCD camera (Kadimisetty, et al, 2016). The main array unit has three 170 μ L reagent reservoirs with sealing caps connected to a common downstream microfluidic channel (Figure 1). Solutions in the reservoirs flow into and fill the 160 μ L detection channel under hydrostatic pressure. Initially, the insert caps seal the

reservoirs. Flow of sample and reagents commences by removing the cap to drain the prefilled reservoir into the detection channel. To run the assay the operator releases the reagents in sequence by removing the inserts.

A larger wash reservoir works with a lever-activated platform that holds the sensor array, wash reservoirs and waste tank at the bottom (Figure 1B). Wash reservoirs also employ custom fit inserts to turn flow on and off. Changing the lever to wash position tilts the sensor array 25° to wash unused immunoreagents to waste.

The sensors in the array have antibodies attached to them to capture the protein analytes from the sample. Assays proceed by allowing sample to fill the detection chamber for an incubation period in which antibodies capture the analytes, then sequential washing, adding 100 nm RuBPY-silica-antibody detection nanoparticles, washing, and incubating. At this point the RuBPY-silica-antibody particles have bound onto the sensors sites that have previously bound analyte proteins in a sandwich immunoassay. Finally TPrA co-reactant is added to fill the detection channel and 1.2 V is applied by the supercapacitor for 30 s. ECL light is initiated from RuBPY in the silica nanoparticles by electrochemical oxidation with TPrA co-reactant, and light is detected by a CCD camera. The supercapacitor is recharged using a small solar panel and a cell phone light.

This immunoarray was tested by detecting three prostate cancer biomarker proteins in serum. The proteins were prostate specific antigen (PSA), prostate specific membrane antigen (PSMA), and platelet factor-4 (PF-4), and assays were completed in 35 min. Detection limits of 0.3-0.5 pg mL⁻¹ for the 3 proteins in undiluted calf serum were found, and the dynamic range is consistent with the levels of these proteins in blood of cancer patients and cancer-free individuals. Assays of 6 prostate cancer patient serum samples gave good correlation with conventional single protein immunoassays (Kadimisetty, et al., 2016). Results suggest successful 3D-printing of major components of a very low cost portable immunoarray device (€0.90 in materials) with replaceable single-use electrode array (€0.20 in materials) for sensitive, accurate detection of proteins in biological samples. Assays cost ~€0.50 each in expendable reagents. Power is supplied by a portable Cellergy, 2.1 V, 80 mF supercapacitor (€10) with a Sparkfun, 0.45 W, 94 mA solar panel (€12) for recharging. The entire immunoarray with power supply costs ~€25, not including the CCD camera. A drawback for point-

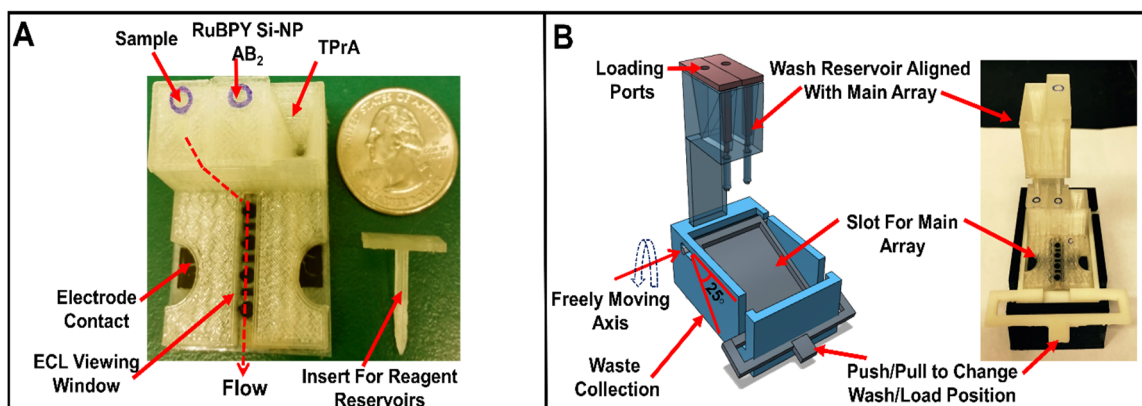


Figure 1: 3D-printed main array and wash reservoir module. (A) Basic array showing three reagent reservoirs equipped with inserts along with flow path for reagents to reach microfluidic channel. (B) Wash reservoir module (1B Left) 3D model showing freely moving lever to change between wash and load position along with wash reservoirs aligned with main array, (1B Right) assembled immunosensor setup with both main array and wash module.

of-care (POC) applications is the lack of automation. Nevertheless, this prototype suggests that 3D-printing will be amenable to more sophisticated immunosensor devices that can be automated (Kadimisetty, et al., 2015).

2.2 Transparent 3D-Printed Devices for ECL Detection

FDM printers produce opaque finishes unsuitable for a closed optical detection chamber. Thus, we designed and printed a prototype ECL sensor device using a Form1+ 3D printer (Formlabs) and clear methacrylate-based resin (Bishop, et al., 2015). Uncured resin was removed by forcing isopropanol through the device channels and then submerging in isopropanol for 10 s. The device was polished using abrasive papers, rinsed with water and dried, then spray-coated with clear acrylic (Krylon, Cleveland, OH) to achieve high clarity. Flow devices were designed with 800 μm diam. channels featuring an oval opening and screw-in inlet and outlet lines to introduce solutions (Figure 3).

We first ascertained that the electrochemical cell in this device gave theoretical voltammetry for standard redox couples that was not influenced by location in the flow channel. We then did simple experiments to demonstrate ECL detection on working electrodes through the clear plastic cell windows. Oxidation of TPA leads to the formation of cation radicals ($\text{TPA}^{\bullet+}$) and free radicals (TPA^{\bullet}) that react with soluble $[\text{Ru}(\text{bpy})_3]^{2+}$ (as well as the RuBPY-silica in the earlier example) to generate electronically excited $[\text{Ru}(\text{bpy})_3]^{2+*}$ that emits ECL light at 610 nm. The 3D-printed channel with integrated electrodes was placed under a CCD

camera housed in a lightproof box to measure ECL (Figure 4). At potential +0.95 V vs. Ag/AgCl, images for 10 min exposure time were clearly visible. Increasing concentrations of the $[\text{Ru}(\text{bpy})_3]^{2+}$ in the reaction mixture gave increased ECL. This simple device and experiments established the technology to design and 3D print ECL based biosensor arrays.

2.3 Prototype Automated 3D-Printed ECL Immunosensor

We then developed a 3D printed array with automated microprocessor controlled sample and reagent delivery. Using the Form 1+ 3D printer we printed a unibody optically clear ECL microfluidic array (Figure 5A) with 5 reagent reservoirs leading into a common microfluidic serpentine channel. The channel addresses an underlying 32-microwell array filled with upright single-wall carbon nanotubes with attached antibodies for simultaneous detection of multiple proteins (Figure 5B). The device is 6.5 x 3.0 x 0.5 mm (L x W x H) and takes 1.5 hours to print at €1.2 per array. The maximum volume of reagent chambers is $\sim 150 \mu\text{L}$ and total volume of the serpentine channel $\sim 140 \mu\text{L}$. Three micropumps are connected to the 3 inlets of the array to pump sample and reagents sequentially from the 5 chambers (Figure 5A) to the detection channel to complete a sandwich immunoassay. Complete automation is achieved by programming micropumps with an Arduino microcontroller to run the assay protocol. The serpentine channel is 3D printed to be open on one side with dimensions 1.2 x 0.15 cm L x W, and 350 μm thick. A tiny groove inside the channel houses a stainless steel wire to serve as a counter

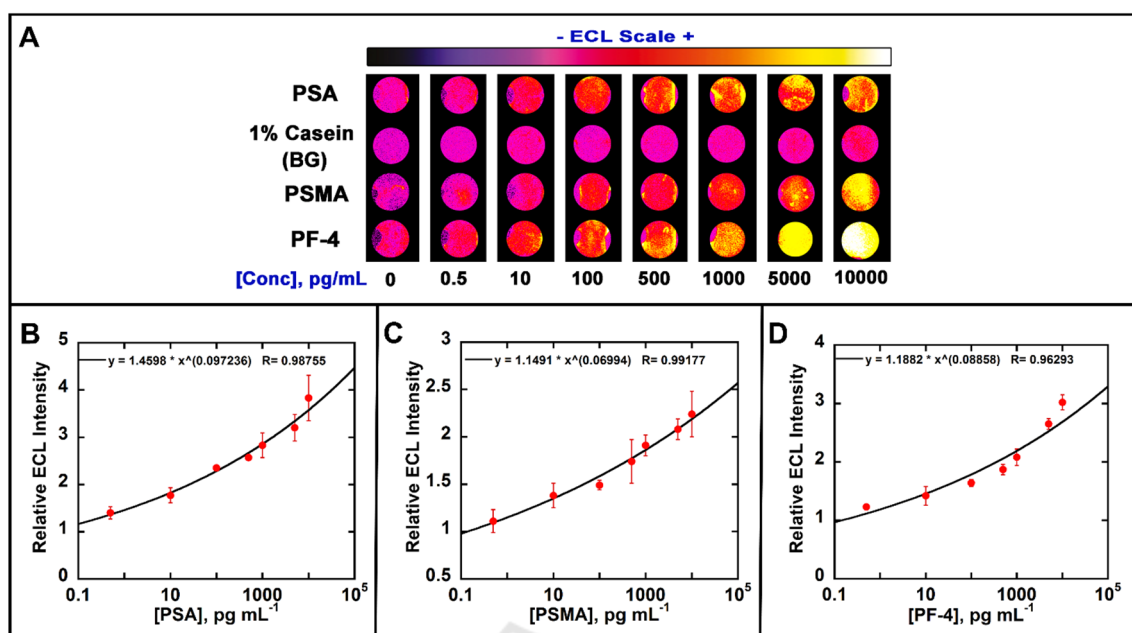


Figure 2: Calibration data from the 3D printed gravity fed immunoarray for 3 proteins in undiluted calf serum showing influence of biomarker protein concentration on ECL response: (A) Recolorized ECL images of 8 arrays with showing increase in ECL intensity with increased concentration. ECL signals digitized for (B) PSA, (C) PSMA and (D) PF-4 in calf serum. Error bars show standard deviation for $n = 4$. Reprinted with permission from Kadimisetty, K., et al., 2016, Copyright Elsevier 2016.

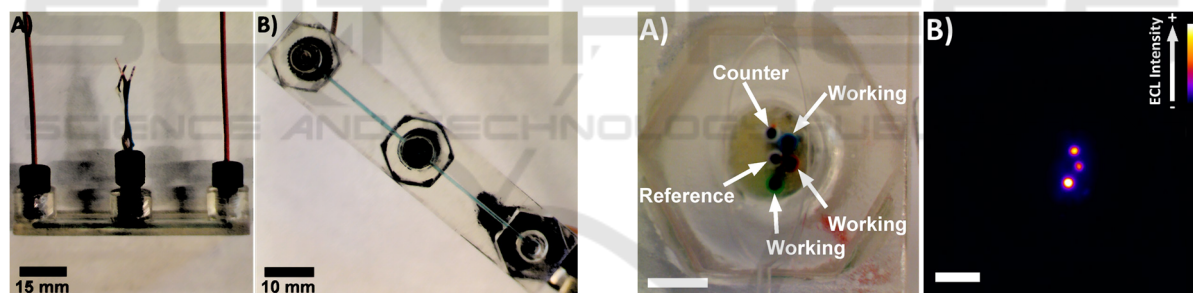


Figure 3: Clear 3D-printed fluidic device with incorporated electrodes for ECL detection. A) Side view equipped with threaded nuts and tubing for inlet/outlet access to the 730 μm fluidic channel and a threaded nut in the center through which Ag/AgCl reference and graphite working and counter electrodes are integrated. B) Bottom view of device, with electrodes on right. Reprinted with permission from Bishop, G.W. et al., 2016, Copyright Amer. Chem. Soc. 2016.

Figure 4: Photographs of 3-working electrode array incorporated into the 3D-printed channel in figure 3. A) Bottom view of 0.5 mm Ag/AgCl reference, 0.5 mm graphite counter and three graphite working electrodes; B) ECL response from electrode array in 180 μM [Ru(bpy)₃]²⁺ in 0.2 M phosphate buffer with 100 mM TPrA. Scale bars represent 3 mm. Reprinted with permission from Bishop, G.W. et al., 2016, Copyright Amer. Chem. Soc. 2016.

electrode. A pyrolytic graphite wafer was patterned with microwells using an inkjet printer (Figure 1B) as the working electrode to produce ECL. This wafer was attached to the open side of the serpentine channel using high tact silicone spray adhesive. The resulting chip defines 32 microwells with 4 spots per turn of the serpentine channel.

Prior to attaching the processed PG chip to the array, upright single wall carbon nanotube forests

were grown in each microwell, followed by chemically linking capture antibodies (Ab_1) to the carboxylated nanotube ends (Kadimisetty, et al., 2015). This Ab_1 coated surface is then exposed to incoming proteins in serum pumped by micropump 1 from chamber 1 during the assay (Figure 5A). Then pumping stops for a 15 min incubation followed by pumping wash buffer from chamber 2. Later micropump 2 is initiated by the program to

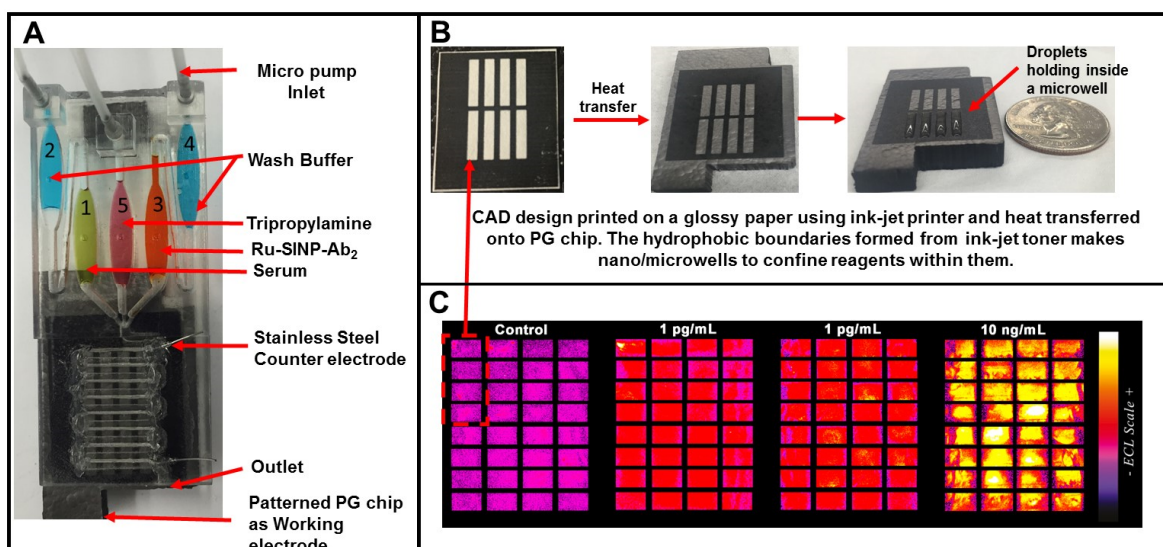


Figure 5: Prototype 3D printed automated immunoarray and proof-of-concept data: (A) Full array with reagent, sample and buffer reservoirs, and serpentine channel covering a series of microwells for ECL generation; (B) the process of forming microwells on the pyrolytic graphite wafer; (C) recolorized 4-array illustration of detection of prostate specific antigen in serum at 0, 1 and 10 pg/mL PSA concentrations.

pump the 100 nm RuBPY-SiNP-Ab₂ detection beads from chamber 3 to the array with captured proteins. RuBPY-SiNP-Ab₂ are then incubated for 15 min, followed by washing unused label particles using wash buffer from chamber 4 to complete the Ab₁-protein-Ab₂ sandwich on the sensors. Then, the ECL generating reagent (350 mM tripropylamine (TrPA) with 0.05% Tween-20 (T20) and 0.05% Triton-X in 0.2 M phosphate buffer) is pumped into the detection chamber from chamber 5. ECL is then generated using a tiny Cellergy supercapacitor applying 1.5 V for 120 s with light captured by a CCD camera in a dark box.

Proof-of-concept experiments on this array showed moderate reproducibility with RSD's $\leq 17\%$ from spot-to-spot ($n=32$) and array-to-array $\leq 13\%$ (Figure 1C). Protocol and printing optimizations are currently underway to improve these RSDs, and to enable reliable multiplexing. Nevertheless, these experiments establish that the automated 3D-printed device can be used for relatively sensitive protein detection. The entire immunoarray was built for ~€250 with three micropumps (€200), an Arduino microcontroller (€30), a supercapacitor (€10) and a 3D printed array including the PG chip (€7). The 3D-printed component cost less than €1 and can be disassembled. The 3D-printed array can be disposable, or regenerated and reused. The CCD camera is of course reusable, but we are also exploring cheaper alternatives.

3 CONCLUSIONS

Our exploratory work described above suggests that low cost 3D printers provide excellent tools to build the molecular diagnostic devices of the future. First, we have fabricated a viable 3D-printed gravity fed immunoarray to detect 3 proteins with better detection limits than most commercially available protein assays. Second, we have developed an approach capable of fabricating closed microfluidic devices that can measure ECL, and realized a prototype automated 3D-printed immunoarray capable of low concentration protein detection. Future applications of the latter device are planned for sensitive detection of 10 proteins in serum.

Universal protein-centered cancer diagnostics promises to decrease overall cancer mortality by earlier detection and molecular therapy monitoring leading to better patient prognoses (Hanash, et al., 2011, Rusling, et. al. 2010). However, widespread translation of these technologies into the clinic will require cheap, reliable, sensitive, automated multiplexed protein detection devices. As we can expect further advances in feature resolution and speed (Tumbleston, J. R., 2015), 3D printing may grow to become a major approach for fabrication of bioanalytical measurement devices.

ACKNOWLEDGEMENTS

This work was supported financially by grants No. EB016707 and EB014586 from the US National Institute of Biomedical Imaging and Bioengineering (NIBIB), NIH.

REFERENCES

- Bishop, G. W., et al., 2015. 3D-Printed Fluidic Devices for Nanoparticle Preparation and Flow-Injection Amperometry Using Integrated Prussian Blue Nanoparticle-Modified Electrodes, *Anal. Chem.* 87, 5437-5443.
- Bishop, G. W., et al., 2016, Electrochemiluminescence at Bare and DNA-Coated Graphite Electrodes in 3D-Printed Fluidic Devices, *ACS Sensors*, in press.
- Coskun, A. F., Wong, J., et al., 2013. A personalized food allergen testing platform on a cellphone, *Lab Chip*. 13, 636-640.
- Coskun, A. F., Nagi, R., et al. 2013. Albumin testing in urine using a smart-phone, *Lab Chip*. 13, 4231-4238.
- Erkal, J. L., et al. 2014. 3D printed microfluidic devices with integrated versatile and reusable electrodes, *Lab Chip*. 14, 2023-2032.
- Forster, R. J., et al., 2009. Electrogenerated chemiluminescence, *Annu. Rev. Anal. Chem.* 2, 359-385.
- Gross, B. C., et al., 2014. Evaluation of 3D printing and its potential impact on biotechnology and the chemical sciences, *Anal. Chem.* 86, 3240-3253.
- Hanash, S. M., et al. 2011. Emerging molecular biomarkers—blood-based strategies to detect and monitor cancer, *Nature Rev. Clin. Oncol.* 8, 142-150.
- Kadimisetty, K., et al., 2015. Automated Multiplexed ECL Immunoarrays for Cancer Biomarker Proteins, *Anal. Chem.* 87, 4472-4478.
- Kadimisetty, K., et al. 2016, 3D-Printed Supercapacitor-Powered Electrochemiluminescent Protein Immunoarray, *Biosens. Bioelectron.*, 77, 188-193.
- Kohane, I. S. 2015. Ten Things We Have To Do To Achieve Precision Medicine, *Science*. 349, 37-38.
- Meng, C., et al., 2015. 3D printed microfluidics for biological applications, *Lab on Chip*, 15, 3627-3637.
- O'Neill, P. F., et al. 2014. Advances in three-dimensional rapid prototyping of microfluidic devices for biological applications. *Biomicrofluidics* 8, 052112.
- Roda, A., et al., 2014. Integrating Biochemiluminescence Detection on Smartphones: Mobile Chemistry Platform for Point-of-Need Analysis, *Anal. Chem.* 86, 7299-7304.
- Rusling, J. F., et al., 2010. Measurement of Biomarker Proteins for Point-of-Care Early Detection and Monitoring of Cancer, *Analyst*. 135, 2496-2511.
- Su, C., Hsia, S., Sun, Y., 2014. Three-dimensional printed sample load/inject valves enabling online monitoring of extracellular calcium and zinc ions in living rat brains, *Anal. Chim. Acta.* 838, 58-63.
- Tumbleston, J. R., et al., 2015. Continuous liquid interface production of 3D objects, *Science*, 347, 1349-1352.
- Wei, Q., Nagi, R., et al., 2014. Detection and Spatial Mapping of Mercury Contamination in Water Samples Using a Smart-Phone, *ACS Nano.* 8, 1121-1129.
- Wei, Q., Luo, W., et al., 2014. Imaging and Sizing of Single DNA Molecules on a Mobile Phone, *ACS Nano.* 8, 12725-12733.